doi:10.1093/jmcb/mjab073
Published online November 9, 2021

Article

The regulatory subunits of PI3K, p85α and p85β, differentially affect BRD7-mediated regulation of insulin signaling

Junsik M. Lee, Renyan Liu, and Sang Won Park*

Division of Endocrinology, Boston Children's Hospital, Harvard Medical School, Boston, MA 02115, USA
* Correspondence to: Sang Won Park, E-mail: sangwon.park@childrens.harvard.edu

Edited by Feng Liu

Bromodomain-containing protein 7 (BRD7) has been shown to interact with the regulatory subunit of phosphatidylinositol 3-kinase (PI3K), p85, in the insulin signaling pathway. Here, we show that upregulation of hepatic BRD7 improves glucose homeostasis even in the absence of either p85 isoform, p85α or p85β. However, BRD7 leads to differential activation of downstream effector proteins in the insulin signaling pathway depending on which isoform of p85 is present. In the presence of only p85α, BRD7 overexpression increases phosphorylation of insulin receptor (IR) upon insulin stimulation, without increasing the recruitment of p85 to IR substrate. Overexpression of BRD7 also increases activation of Akt in response to insulin, but does not affect basal phosphorylation levels of Akt. Meanwhile, the phosphorylation of glycogen synthase kinase 3β (GSK3β) is increased by overexpression of BRD7. On the other hand, in the presence of only p85β, BRD7 overexpression does not affect phosphorylation levels of IR, and Akt phosphorylation is not affected by insulin stimulation following BRD7 upregulation. However, BRD7 overexpression leads to increased basal phosphorylation levels of Akt and GSK3β. These data demonstrate that BRD7's action on glucose homeostasis does not require the presence of both p85 isoforms, and p85α and p85β have unique roles in insulin signaling in the liver.

Keywords: PI3K, BRD7, Akt, insulin signaling

Introduction

Type 2 diabetes is a disease characterized by impaired insulin sensitivity and progressive development of hyperglycemia, which increases the risk of many other complications, including cardiovascular disease, stroke, blindness, and kidney failure (Forbes and Cooper, 2013; Park and Ozcan, 2013; DeFronzo et al., 2015). Obesity is one of the main contributing factors behind the development of type 2 diabetes. The rising incidence of obesity and type 2 diabetes has become a major public health issue worldwide, especially over the last few decades. Despite enormous efforts dedicated to unraveling the insulin signaling pathway, the understanding of molecular mechanisms underlying insulin resistance in obesity still remains incomplete.

Received July 27, 2021. Revised September 15, 2021. Accepted September 24, 2021.

Bromodomain-containing protein 7 (BRD7) is a member of the bromodomain-containing protein family, initially reported in nasopharyngeal carcinoma cells (Zhou et al., 2004). Since then, it has been shown that BRD7 interacts with p53 (Burrows et al., 2010; Drost et al., 2010; Mantovani et al., 2010) and BRCA-1 (Harte et al., 2010) and plays a role as a tumor suppressor. In addition, it has been found to participate in many other cellular processes. For instance, BRD7 promotes the association between vitamin D receptor and PBAF chromatin remodeling complex to restore impaired β cell function in genetically obese and diabetic mouse models (Wei et al., 2018). In our previous work, we demonstrated that hepatic BRD7 levels are reduced in obese mice, and restoration of BRD7 significantly improves glucose homeostasis in both genetically obese *ob*/*ob* mice and high-fat diet (HFD)-induced obese mice (Park et al., 2014; Lee et al., 2019). We showed that BRD7 interacts with the regulatory subunits of phosphatidylinositol 3-kinase (PI3K), p85α and p85β, and increases their nuclear translocation (Chiu et al., 2014; Park et al., 2014). The BRD7–p85 interaction, in turn, increases the nuclear translocation of the spliced form of X-box binding protein 1 (XBP1s), a transcription factor that

plays a key role in the endoplasmic reticulum (ER) homeostasis. Decreased hepatic BRD7 level in obesity leads to decreased nuclear translocation of XBP1s and consequently increases ER stress levels, leading to disturbed glucose homeostasis (Park et al., 2010, 2014). BRD7 also increases the phosphorylation of glycogen synthase kinase 3β (GSK3β; Golick et al., 2018). Of note, increased phosphorylation of GSK3β following overexpression of BRD7 occurs even in the absence of Akt (Golick et al., 2018). On the other hand, overexpression of BRD7 leads to increased phosphorylation of eukaryotic translation initiation factor 4E (eIF4E)-binding protein 1 (4E-BP1), which relieves inhibition of eIF4E, but only in the presence of Akt (Golick et al., 2018).

p85α and p85β exist as monomers (Ueki et al., 2002) or p85α–p85β heterodimers (Park et al., 2010), which are dissociated by insulin stimulation (Park et al., 2010). The p85 monomers compete with the p85–p110 complex for the p85-docking site on insulin receptor substrate (IRS) proteins (Ueki et al., 2002). There have been a few reports that suggested different roles of p85α and p85β. For example, it has been shown that the loss of p85α, but not p85β, impairs the development and proliferation of B cells (Oak et al., 2009). In the context of cancer, it has been shown that p85α acts as a tumor suppressor, while p85β induces tumor formation (Vallejo-Diaz et al., 2019). Based on these findings, we raised the possibility of differential roles of p85α and p85β in the BRD7-mediated regulation of insulin signaling and glucose homeostasis.

Results

p85 is required for stable BRD7 expression

We previously reported that hepatic BRD7 levels are reduced in genetically obese *ob*/*ob* and HFD-induced obese mice (Park et al., 2014). We sought to investigate the cause of the reduction in BRD7 levels in obesity. Based on our previous report that showed the interaction between BRD7 and p85α/β (Chiu et al., 2014; Park et al., 2014), we questioned whether hepatic p85 levels have any effect on BRD7 expression. To answer this question, we first measured p85 protein levels in the liver of wild-type C57BL/6J (WT) mice that were fed on either a normal chow diet (NCD) or HFD for 30 weeks. The western blotting results showed that p85 levels are reduced in the liver of HFD-fed mice (Figure 1A) compared to NCD-fed mice at the 6-h-fasted state. There was no difference in p85 and BRD7 mRNA levels between the two groups (Figure 1B). Based on these observations, we asked whether the reduced p85 protein levels are correlated with BRD7's stability. To test this possibility, we infected mouse embryonic fibroblasts (MEFs) derived from WT or p85α/β double knockout (p85DKO) mice with an adenovirus that expresses BRD7 (Ad-BRD7) and used an adenovirus that expresses eGFP (Ad-eGFP) as a control. The results showed that BRD7 is expressed at a higher level in WT MEFs compared to p85DKO MEFs (Figure 1C). To confirm the results in liver cells, we isolated primary hepatocytes from WT mice and infected the cells with a mixture of adenoviruses that express shRNA sequences specific for p85α and p85β. Ad-LacZshRNA was used as a control. We coinfected the cells with Ad-BRD7 or Ad-LacZ (control). Western blotting results showed reduced BRD7 expression levels when p85 was knocked down (Supplementary Figure S1A). Furthermore, we isolated primary hepatocytes from WT (control) and $p85\alpha^{flox/flox}p85\beta^{-/-}$ mice and infected the cells with an adenovirus that expresses Cre (Ad-Cre). The results showed decreased BRD7 expression levels in the cells from $p85\alpha^{flox/flox}p85\beta^{-/-}$ mice (Supplementary Figure S1B). Conversely, reinstating p85α in primary hepatocytes that lack p85α/β by infecting the cells with Ad-p85α led to increased BRD7 levels (Supplementary Figure S1C). Lastly, we examined the expression levels of endogenous BRD7 in the liver of WT mice or mice that lack p85α or p85β. We immunoprecipitated (IP) BRD7 from total lysate obtained from the liver using an antibody specific to BRD7 and immunoblotted for BRD7. The result showed that decreased p85 levels lead to decreased endogenous BRD7 levels (Supplementary Figure S1D).

Next, we sought to examine the degradation rate of BRD7 protein in these two cell types. To do this, we infected WT and p85DKO MEFs with Ad-BRD7 at the same dose and treated the cells with 40 μM cycloheximide for 3 h to inhibit global protein translation or DMSO as a control. BRD7 expression levels in DMSO-treated p85DKO MEFs were significantly lower than that in DMSO-treated WT MEFs and comparable to that observed in cycloheximide-treated WT MEFs (Figure 1D). Next, we sought to compare the half-life of BRD7 in the presence or absence of p85s. For this purpose, we infected WT and p85DKO MEFs with Ad-BRD7 and treated them with 40 μM cycloheximide for various time points. Western blotting results showed that the half-life of BRD7 in WT MEFs is ∼75 min (Figure 1E), whereas the half-life of BRD7 in p85DKO MEFs is ∼30 min in the absence of p85s (Figure 1F).

To directly show that decreased BRD7 expression in p85DKO MEFs is due to the lack of p85, we investigated whether restoring p85 in p85DKO MEFs would stabilize BRD7 and, therefore, increase BRD7 expression levels. For this, we infected WT and p85DKO MEFs with Ad-BRD7 alone or together with either Ad-p85α or Ad-p85β. Ad-eGFP was used as a control such that all cells were infected with the same total amount of adenovirus. Coinfecting p85DKO MEFs with Ad-BRD7 and Ad-p85α resulted in a robust increase of BRD7 expression (Figure 1G). The same pattern was observed when p85DKO cells were coinfected with Ad-BRD7 and Ad-p85β (Figure 1H).

BRD7 improves glucose homeostasis in the presence of p85α alone

We previously showed that restoration of BRD7 in the liver of obese mice improves glucose homeostasis (Park et al., 2014). Based on our results that show an important role of p85 in sustaining BRD7 expression, we questioned whether BRD7 can still improve glucose homeostasis when one of p85 isoforms is absent. To answer this question, we placed p85β knockout ($p85\beta^{-/-}$) mice on HFD (45% kcal from fat) for 7–8 weeks after weaning. We then overexpressed BRD7 or LacZ as a control in

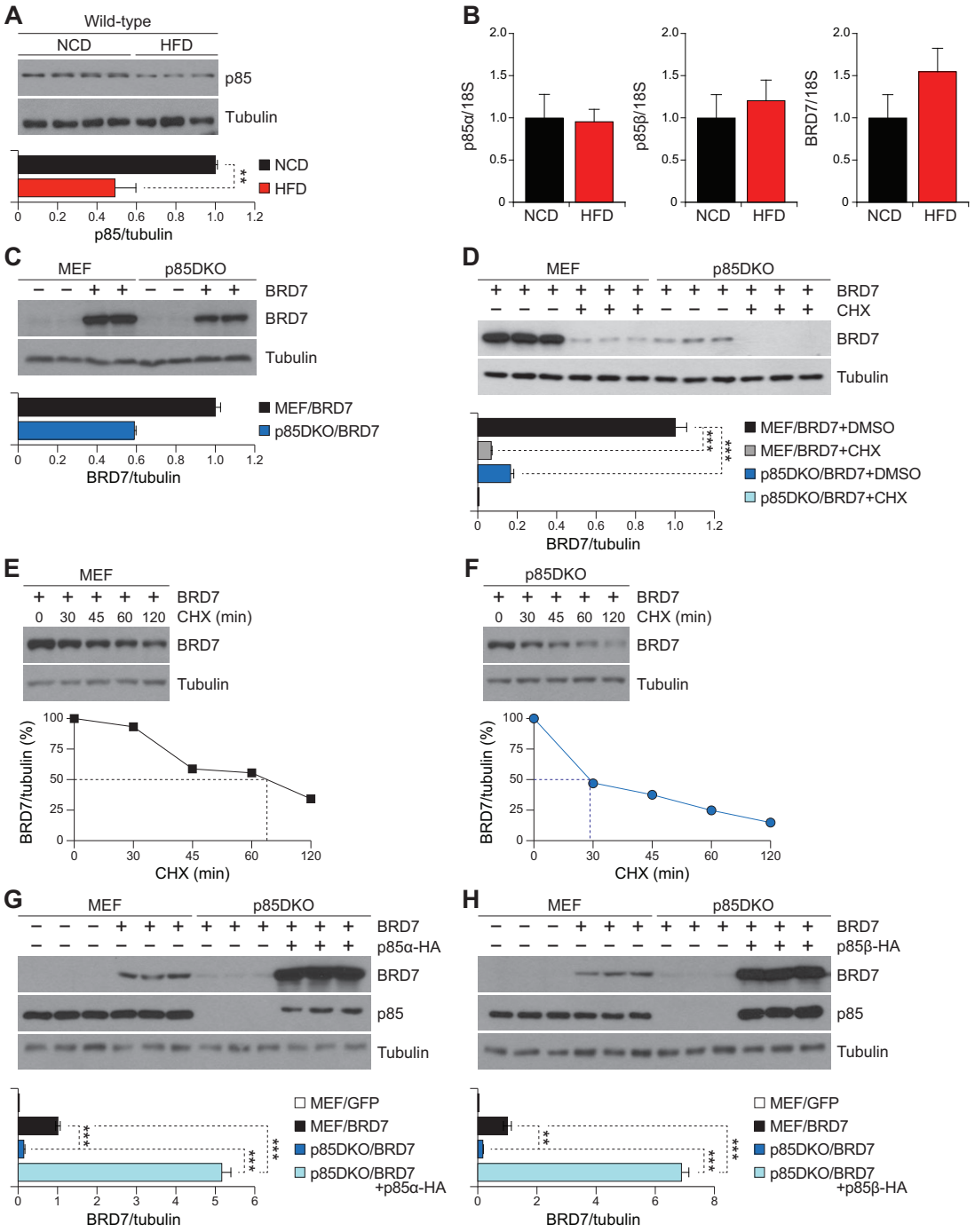

Figure 1 p85 is required for stable BRD7 expression. (**A**) Western blotting for p85 in the liver of wild-type mice after 30 weeks of NCD or HFD feeding. (**B**) Relative mRNA levels of *PIK3R1* (p85α), *PIK3R2* (p85β), or *BRD7* normalized to 18S in the liver of wild-type mice after 30 weeks of NCD or HFD feeding ($n = 3$). (**C**–**H**) Western blotting was performed with the indicated antibodies. Cells not infected with Ad-BRD7 or Ad-p85 were infected with Ad-eGFP as a control. (**C**) Wild-type MEFs (MEF) and p85DKO MEFs (p85DKO) were infected with Ad-BRD7. (**D**) MEF and p85DKO were infected with Ad-BRD7 and treated with 40 μM cycloheximide (CHX) or DMSO as a control for 3 h. (**E**) MEF were infected with Ad-BRD7 and treated with 40 μM CHX or DMSO as a control for the indicated time periods. (**F**) p85DKO were infected with Ad-BRD7 and treated with 40 μM CHX or DMSO as a control for the indicated time periods. (**G**) MEF and p85DKO were infected with Ad-BRD7 or Ad-p85α as indicated. (**H**) MEF and p85DKO were infected with Ad-BRD7 or Ad-p85β as indicated. For all graphs, Student's *t*-test was used to determine *P*-values. Error bars represent SEM. $^{**}P < 0.01$, $^{***}P < 0.001$. Analysis was performed only for blots with $n \geq 3$.

the liver of mice by tail vein injection of Ad-BRD7 or Ad-LacZ. The Ad-BRD7-injected mice displayed decreased blood glucose levels on Day 8 postinjection compared to the Ad-LacZ-injected group (Figure 2A). Glucose tolerance test (GTT) performed on Day 4 postinjection showed a significant improvement in glucose disposal rate in the Ad-BRD7-injected group compared to the Ad-LacZ-injected group, revealing that BRD7 can improve glucose tolerance in the presence of only p85α (Figure 2B). Insulin tolerance test (ITT) performed on Day 6 postinjection revealed an improvement in whole-body insulin sensitivity in the Ad-BRD7-injected group (Figure 2C).

BRD7 improves insulin signaling in the presence of p85α alone

We sought to investigate whether hepatic insulin receptor (IR) signaling is altered by BRD7 overexpression in the presence of p85α alone. For this purpose, we used primary hepatocytes isolated from p85β$^{-/-}$ mice and infected them with either Ad-BRD7 or Ad-eGFP as a control, followed by insulin stimulation for 10 min. Immunoprecipitation experiments showed that the phosphorylation of IR upon insulin stimulation was increased in cells that were infected with Ad-BRD7 compared to that in the Ad-eGFP-infected cells (Figure 3A). However, there was no difference in the recruitment of p85 to IRS1 or IRS2 (Figure 3A) between the Ad-BRD7-infected and Ad-eGFP-infected cells. To examine the activation of IR signaling in the presence of only p85α in an *in vivo* setting, we placed p85β$^{-/-}$ mice on HFD for 7–8 weeks and injected them with Ad-BRD7 or Ad-LacZ as a control through the tail vein. After 8 days, we infused either insulin (1.2 IU/kg) or saline as a control through the portal vein. Western blotting results from liver lysates showed that the phosphorylation levels of IR are slightly increased in response to insulin when BRD7 was upregulated in the liver of p85β$^{-/-}$ mice. No difference was observed in the recruitment of p85 to IRS1 or IRS2 between the Ad-BRD7-injected and Ad-LacZ-injected groups, following insulin stimulation (Figure 3B).

Next, we sought to investigate the effect of BRD7 on Akt phosphorylation in the presence of p85α alone. To answer this question, we first infected the primary hepatocytes isolated from p85β$^{-/-}$ mice with either Ad-BRD7 or Ad-eGFP as a control and then treated the cells with insulin for 10 min. The cells that were infected with Ad-BRD7 showed a greater increase in pAkt308 and pAkt473 phosphorylation following insulin stimulation compared to the Ad-eGFP-infected cells (Figure 4A).

To understand how BRD7 overexpression in the presence of only p85α under an HFD-induced obese condition affects Akt phosphorylation levels in an *in vivo* setting, we performed western blotting using protein lysates obtained from the liver of HFD-fed p85β$^{-/-}$ mice that were injected with Ad-BRD7 or Ad-LacZ as a control through the tail vein and infused with either insulin (1.2 IU/kg) or saline as a control through the portal vein on Day 8 postinjection. The phosphorylation levels of pAkt473 and GSK3β at residue Ser9 (pGSK3β) after insulin stimulation were increased in Ad-BRD7-injected mice compared to that in Ad-LacZ-injected mice (Figure 4B). Next, we questioned whether BRD7 overexpression affects basal phosphorylation levels of Akt and GSK3β. For this, p85β$^{-/-}$ mice were fed on HFD for 7–8 weeks and injected with Ad-BRD7 or Ad-LacZ as a control through the tail vein. Liver tissues were collected on Day 8 postinjection after 6 h of fasting. We performed western blotting using a higher amount of protein to detect the basal levels of phosphorylation without insulin stimulation compared to the amounts of proteins used in Figure 4A and B. The result showed that BRD7 does not increase the basal phosphorylation levels of Akt in the liver of p85β$^{-/-}$ mice without insulin stimulation (Figure 4C). Meanwhile, the basal phosphorylation levels of GSK3β were significantly increased in the Ad-BRD7-injected group compared to that in the Ad-LacZ-injected group (Figure 4D).

p85α is necessary for BRD7-mediated increase in Akt activation in response to insulin

To investigate the effect of BRD7 on glucose homeostasis and insulin signaling in the presence of only p85β, we placed liver-specific p85α knockout (p85α$^{F/F}$Alb-Cre$^{+/-}$, p85αKO) mice on HFD for 7–8 weeks, and then injected them with Ad-BRD7 or Ad-LacZ as a control. The Ad-BRD7-injected mice displayed decreased blood glucose levels after 6 h of fasting on Day 9 postinjection (Figure 5A). GTT performed on Day 4 postinjection showed a significant increase in glucose disposal rate in Ad-BRD7-injected mice compared to that in Ad-LacZ-injected mice (Figure 5B). ITT performed on Day 6 postinjection revealed a significant decrease in the area under the curve (AUC) in Ad-BRD7-injected mice with significantly decreased basal blood glucose levels prior to insulin administration, but there was no difference in the percent change of blood glucose (Figure 5C).

To examine whether hepatic IR signaling is altered by BRD7 overexpression in the presence of p85β alone, we isolated primary hepatocytes from p85αKO mice and infected them with either Ad-BRD7 or Ad-eGFP as a control, followed by insulin stimulation for 10 min. Immunoprecipitation experiments showed no difference in phosphorylation levels of IR between Ad-BRD7-infected and Ad-LacZ-infected groups after insulin stimulation (Figure 6A). There was no difference in the interaction levels between p85 and IRS1 (Figure 6A).

Next, we investigated the phosphorylation levels of Akt in Ad-BRD7-infected p85αKO hepatocytes and observed no significant difference in pAkt308 and pAkt473 between Ad-BRD7-infected and Ad-GFP-infected cells upon insulin stimulation (Figure 6B). To confirm the effect of BRD7 overexpression on Akt phosphorylation levels in the presence of only p85α under HFD-induced obese conditions in an *in vivo* setting, we performed western blotting using protein lysates obtained from the liver of HFD-fed p85αKO mice that were injected with Ad-BRD7 or Ad-LacZ as a control through the tail vein and infused with either insulin (1.2 IU/kg) or saline as a control through the portal vein on Day 8 postinjection. The fold change in

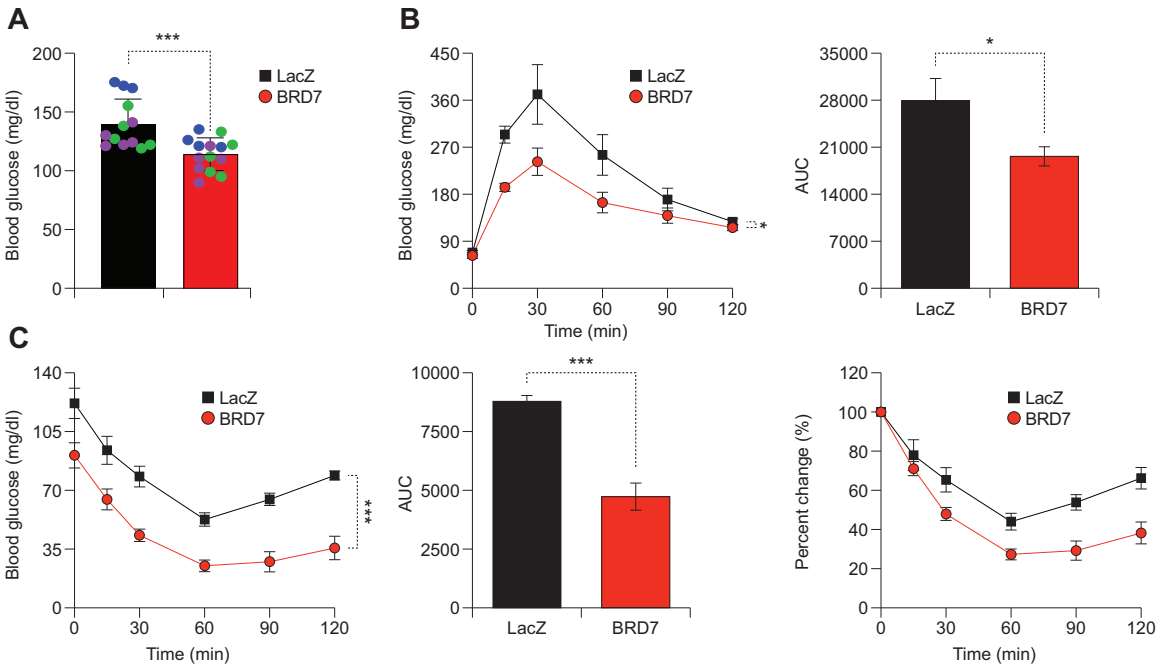

Figure 2 BRD7 improves glucose homeostasis in the presence of p85α alone. (**A**) p85β$^{-/-}$ mice were placed on HFD for 7–8 weeks starting at 4–5 weeks of age and injected with Ad-BRD7 or Ad-LacZ as a control through the tail vein at a dose of 1.5×10^8 (cohort 1, $n = 4$) or 5.0×10^7 (cohort 2, $n = 5$) pfu/g body weight. Blood glucose levels were measured on Day 8 postinjection after 6 h of fasting. Each dot represents an individual mouse. Different colors represent different cohorts. (**B**) GTT (1.5 g/kg, $n = 5$, 5.0×10^7 pfu/g) on Day 4 postinjection (left). AUC (right). (**C**) ITT (1.5 IU/kg, $n = 5$, 5.0×10^7 pfu/g) on Day 6 postinjection (left). AUC (middle). Percent change of initial blood glucose levels (right). For blood glucose levels and AUC, Student's *t*-test was used to determine *P*-values. GTT and ITT were analyzed using two-way repeated measure ANOVA. Error bars represent SEM. *$P < 0.05$, ***$P < 0.001$.

phosphorylation levels of pAkt473 and pAkt308 after insulin stimulation were similar in Ad-BRD7-injected and Ad-LacZ-injected mice (Figure 6C). We examined the basal Akt phosphorylation levels in liver tissues of 6-h-fasted HFD-fed p85αKO mice that were injected with Ad-BRD7 or Ad-LacZ as a control through the tail vein. Western blotting results showed increased pAkt473 and pAkt308 phosphorylation in the Ad-BRD7-injected group compared to that in the group injected with Ad-LacZ (Figure 6D). pGSK3β was also increased in the Ad-BRD7-injected group (Figure 6E). Gene expression of glucose-6-phosphatase (G6P), fructose 1,6-bisphosphatase (F6P), and phosphoenolpyruvate carboxykinase (PEPCK) were not changed by overexpression of BRD7 in the liver of mice that lack either p85α or p85β, at the 6-h-fasted state (Supplementary Figure S2A and B).

Discussion

Hepatic BRD7 levels have been reported to be an important factor in the maintenance of glucose homeostasis in obesity, and BRD7 has emerged as a new player in insulin signaling. BRD7 levels are reduced in the liver of HFD-induced obese mice and genetically obese *ob*/*ob* mice, and restoration of BRD7 in the liver of obese mice improves glucose homeostasis (Park et al., 2014). However, the cause of reduced BRD7 levels in the liver remained unanswered. Here, we report that the presence of either isoform of p85, p85α or p85β, is required to maintain stable expression of BRD7. Lack of p85 leads to decreased expression levels of BRD7, and restoration of either p85α or p85β in cells that lack p85α/β is enough to maintain BRD7 expression induced by Ad-BRD7 infection.

In this report, we focus our study on the effect of lack of either p85α or p85β on BRD7's action in HFD-fed mice. It is interesting to note that the two mouse lines that lack either p85α or p85β in the liver presented different downstream effects in the insulin signaling pathway in response to the upregulation of hepatic BRD7. The blood glucose levels during insulin challenge showed that hepatic p85α, but not p85β, is responsible for interacting with BRD7 to improve insulin sensitivity. This is consistent with the observation that BRD7 overexpression in the liver of p85β$^{-/-}$ mice, but not in a mouse line that lacks p85α, increased sensitivity of the IR–IRS axis and Akt phosphorylation in response to insulin. How does BRD7 mediate phosphorylation of Akt in response to insulin in the presence of only p85α, while p85β does not have a significant effect on Akt phosphorylation by BRD7 upon insulin stimulation? While further investigation is required to answer this question, one possibility can be raised by the fact that p85α is more abundant than p85β (Ueki et al., 2002). p85 monomers that are not bound to p110 compete with p85–p110 dimers for the same

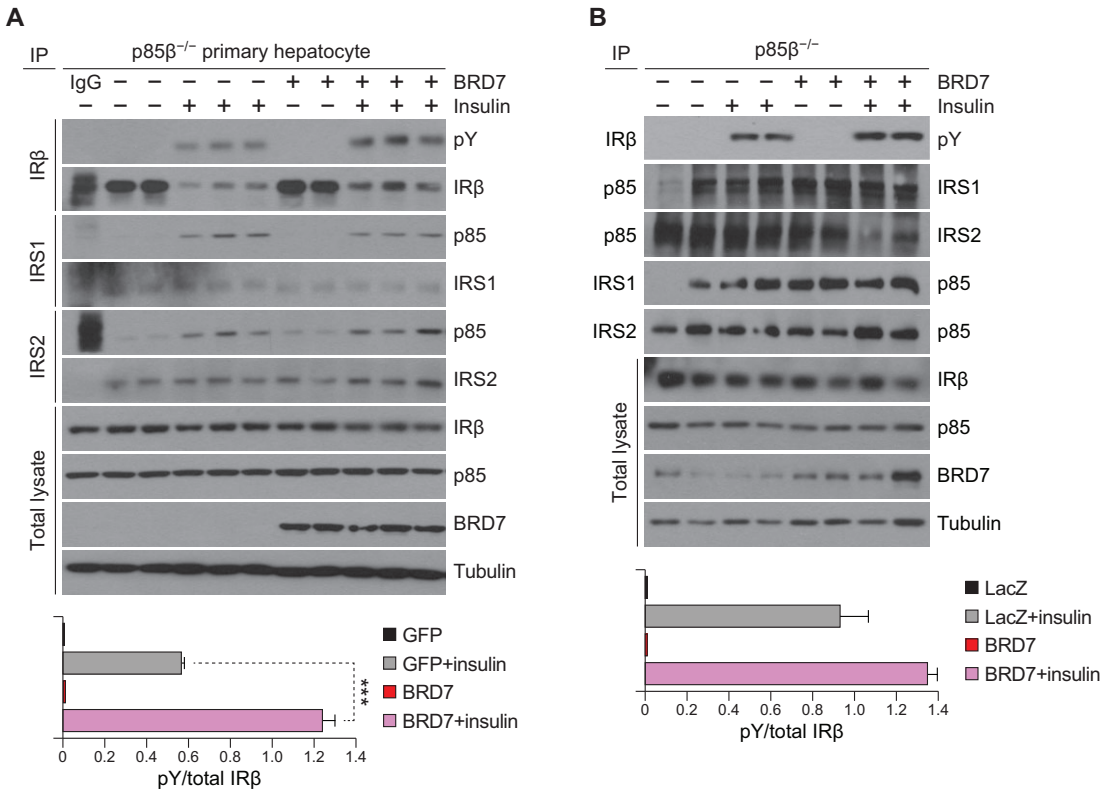

Figure 3 BRD7 improves insulin signaling in the presence of p85α alone. (**A**) Primary hepatocytes were isolated from p85β$^{-/-}$ mice and infected with Ad-BRD7 or Ad-LacZ as a control and stimulated with 100 nM insulin for 10 min. Total cell lysates were IP with the indicated antibodies and immunoblotted with the indicated antibodies. (**B**) p85β$^{-/-}$ mice were placed on HFD for 7–8 weeks starting at 4 weeks of age and injected with Ad-BRD7 or Ad-LacZ as a control through the tail vein at a dose of 1.5×10^8 pfu/g body weight. On Day 8 postinjection, mice were fasted for 6 h and infused with insulin at a dose of 1.2 IU/kg body weight or saline as a control through the portal vein for 3 min. Total lysates from the liver tissues were IP with the indicated antibodies and immunoblotted with the indicated antibodies. For both graphs, Student's *t*-test was used to determine *P*-values. Error bars represent SEM. ***$P < 0.001$. Analysis was performed only for blots with $n \geq 3$.

binding sites on IRS proteins. The binding of p85 monomers to IRS results in sequestration of IRS and suppression of PI3K–Akt signaling (Luo et al., 2005). Perhaps the amount of p85α in p85β$^{-/-}$ mice is sufficient to compete with p85–p110 dimers and inhibit PI3K–Akt signaling. Under such conditions, overexpression of BRD7 would reduce the availability of p85α monomers to bind to IRS proteins, removing the inhibitory role of monomeric p85α. Another possibility is that p85α and p85β have different affinities for the IRS-binding site: p85α may have a higher affinity, resulting in a differential response when BRD7 is upregulated.

We showed that BRD7 increases basal Akt phosphorylation levels in the presence of only p85β, but not when only p85α was present. What would be the explanation for having no effect on Akt phosphorylation when only p85α was present without insulin stimulation? One possible explanation for this observation can be speculated from the fact that p85α forms homodimers in the absence of insulin stimulation, and this p85α homodimer binds to phosphatase and tensin homolog (PTEN), resulting in stabilization of PTEN by protecting it from proteasomal degradation (Cheung et al., 2015). Therefore, the effect of BRD7 on Akt phosphorylation may not be detected because p85α homodimer–PTEN is constantly suppressing PI3K activity in the absence of insulin. Meanwhile, p85β has reduced capability to homodimerize and does not act to stabilize PTEN (Cheung et al., 2015). Therefore, the effect of BRD7–p85β on Akt phosphorylation is observed since the PI3K-suppressing effect of PTEN is reduced in the absence of p85α homodimer.

While BRD7 displays different effects on Akt phosphorylation levels depending on whether p85α or p85β is present, BRD7 increases the phosphorylation of GSK3β independent of p85 isoforms. This is in alignment with our previous report that showed BRD7 increases phosphorylation of GSK3β even in the absence of Akt (Golick et al., 2018). Gluconeogenic gene analysis showed no significant difference upon BRD7 overexpression in the absence of either isoform at a basal state without insulin stimulation. A further detailed investigation is required to understand this mechanism.

It is also important to note that BRD7 regulates Akt activation differentially depending on the cellular environment and

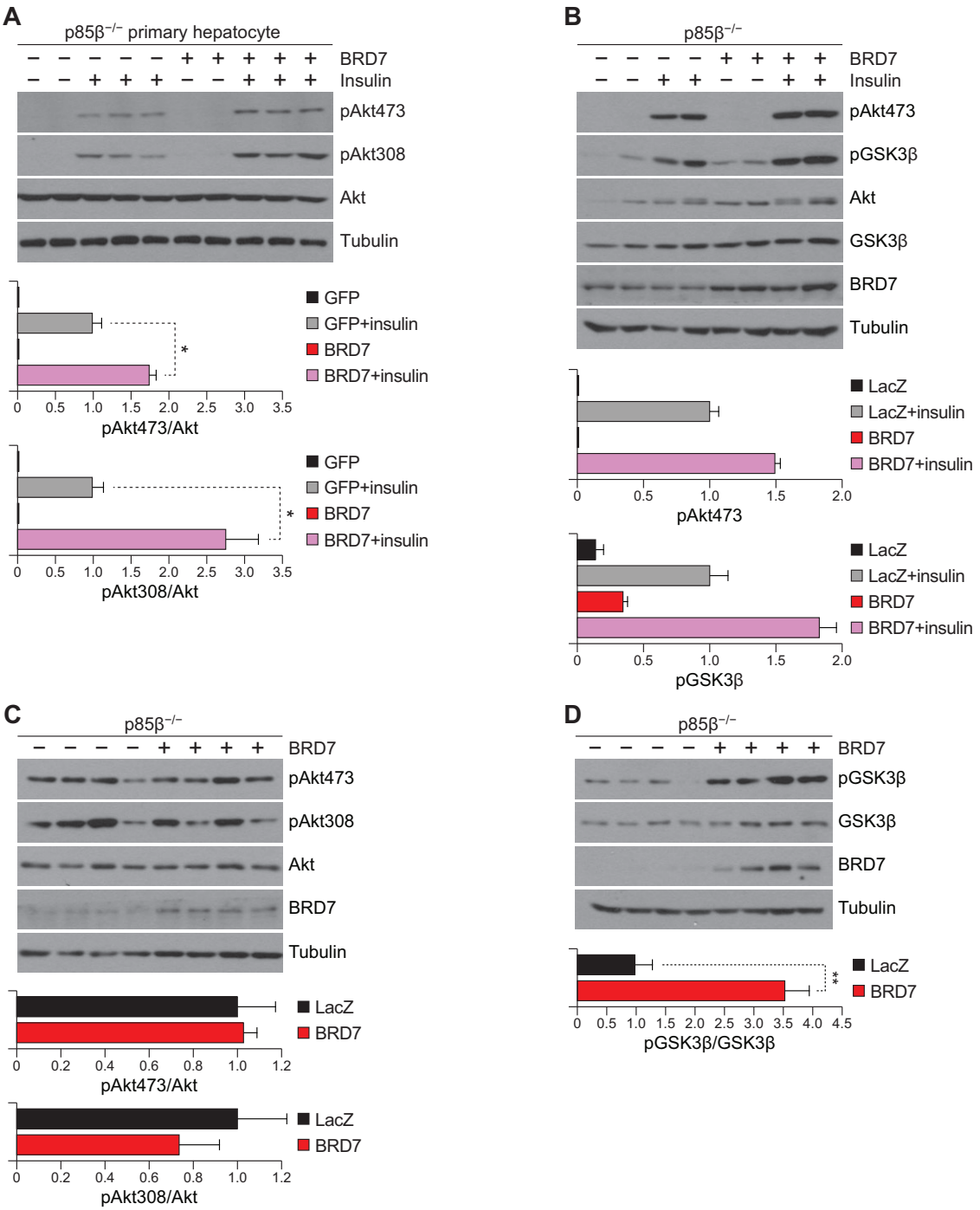

Figure 4 Basal levels of Akt are not affected by BRD7 overexpression in the presence of p85α alone. (**A**) Primary hepatocytes were isolated from p85β$^{-/-}$ mice, infected with Ad-BRD7 or Ad-eGFP as a control, and stimulated with 100 nM insulin for 10 min. Total lysates were analyzed by western blotting with the indicated antibodies. (**B**) p85β$^{-/-}$ mice were placed on HFD for 7–8 weeks starting at 4–5 weeks of age and injected with Ad-BRD7 or Ad-LacZ as a control through the tail vein at a dose of 1.5×10^8 pfu/g body weight. On Day 8 postinjection, mice were fasted for 6 h and infused with insulin at a dose of 1.2 IU/kg body weight or saline as a control through the portal vein for 3 min. Total lysates from the liver were analyzed by western blotting with the indicated antibodies. (**C** and **D**) p85β$^{-/-}$ mice were placed on HFD for 7–8 weeks starting at 4–5 weeks of age and injected with Ad-BRD7 or Ad-LacZ as a control through the tail vein at a dose of 5.0×10^7 pfu/g body weight. Western blotting was performed on total lysates from the liver with the indicated antibodies. (**C**) Phosphorylation levels of Akt from the liver tissues on Day 8 postinjection after 6 h of fasting. (**D**) Phosphorylation levels of GSK3β from the liver tissues on Day 8 postinjection after 6 h of fasting. For all graphs, Student's *t*-test was used to determine *P*-values. Error bars represent SEM. *$P < 0.05$, **$P < 0.01$. Analysis was performed only for blots with $n \geq 3$.

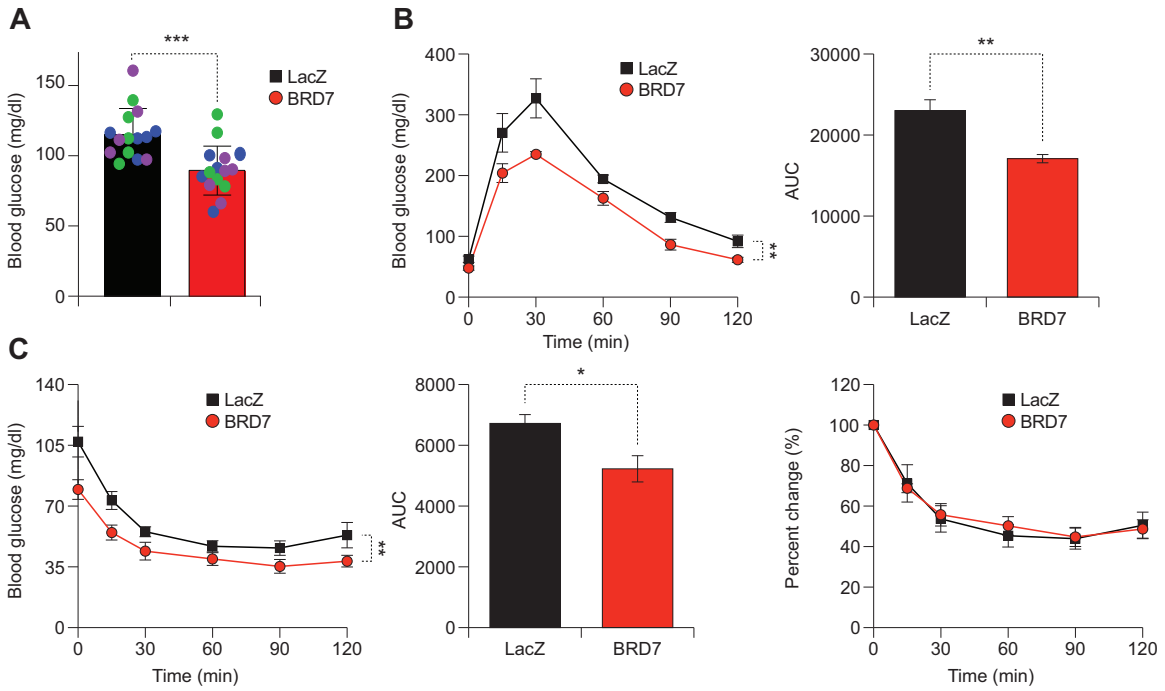

Figure 5 BRD7 improves glucose tolerance in the presence of p85β alone. (**A**) p85αKO mice were placed on HFD for 7–8 weeks starting at 4–5 weeks of age and injected with Ad-LacZ or Ad-BRD7 as a control through the tail vein at a dose of 1.5×10^8 (cohort 1, $n = 5$) or 1.0×10^8 (cohort 2, $n = 3$) pfu/g body weight. Blood glucose levels were measured on Day 9 postinjection after 6 h of fasting. Each dot represents an individual mouse. Different colors represent different cohorts. (**B**) GTT (1.5 g/kg, $n = 5$, 1.5×10^8 pfu/g) on Day 4 postinjection (left). AUC (right). (**C**) ITT (1.2 IU/kg, $n = 5$, 1.5×10^8 pfu/g) on Day 6 postinjection (left). AUC (middle). Percent change of initial blood glucose levels (right). For blood glucose levels and AUC, Student's *t*-test was used to determine *P*-values. GTT and ITT were analyzed using two-way repeated measure ANOVA. Error bars represent SEM. $^*P < 0.05$, $^{**}P < 0.01$, $^{***}P < 0.001$.

abundance of proteins (Park and Lee, 2020). For example, we previously reported that BRD7 interacts with p85 and increases the nuclear import of p85, and BRD7 overexpression increases insulin-stimulated Akt phosphorylation in the liver of *ob*/*ob* mice (Park et al., 2014). The mechanism by which overexpression of BRD7 affects Akt activation in response to insulin in obesity can be speculated from the fact that the p85s exist in excess of the p110 catalytic subunit of PI3K in the liver. Therefore, a reduction in p85 monomers in the cytoplasm by BRD7 would increase the availability of p85–p110 dimers to IRS, resulting in the BRD7-mediated enhancement of Akt phosphorylation. On the other hand, in the HeLa cervical cancer cell line, the nuclear import of p85α by BRD7 destabilizes the p110 subunit, and overexpression of BRD7 attenuates PI3K signaling and Akt phosphorylation (Chiu et al., 2014). Additionally, it is interesting to note that mutations of p85α in endometrial cancer have been shown to either prevent p85α from forming homodimers or disrupt the interaction between p85α homodimers and PTEN, both of which lead to degradation of PTEN and increase of PI3K activity (Cheung et al., 2015). It would require further investigation to understand how BRD7 acts differently in a cancerous state.

p85 signaling is complex and displays various functions depending on genotypes, tissues, and cells types. For instance, whole-body p85α knockout and hepatic p85α knockout mice have improved insulin sensitivity (Mauvais-Jarvis et al., 2002; Taniguchi et al., 2006). Downregulation of p85α in pancreatic β cells of heterozygous Akita mice leads to delayed development of diabetes (Winnay et al., 2014). On the other hand, brown adipose tissue-specific knockout of p85α in HFD-fed mice improves thermogenic functionality and protects against the development of insulin resistance (Gomez-Hernandez et al., 2020). PI3K activity has been shown to be decreased in skeletal muscle of type 2 diabetic and obese individuals (Bandyopadhyay et al., 2005). Overexpression of p85 in the liver of obese mice leads to improved glucose homeostasis (Park et al., 2014). In this report, we showed that the two isoforms of p85 display different roles in regards to BRD7's activity in IR signaling and Akt activation (Figure 7). Our work provides a strong foundation for elucidating the molecular basis for BRD7's action in regulating glucose homeostasis and understanding insulin signaling in obesity.

Materials and methods

Cell culture

Cells were maintained in tissue-culture treated plates (Corning, CLS430167) in Dulbecco's modified eagle medium

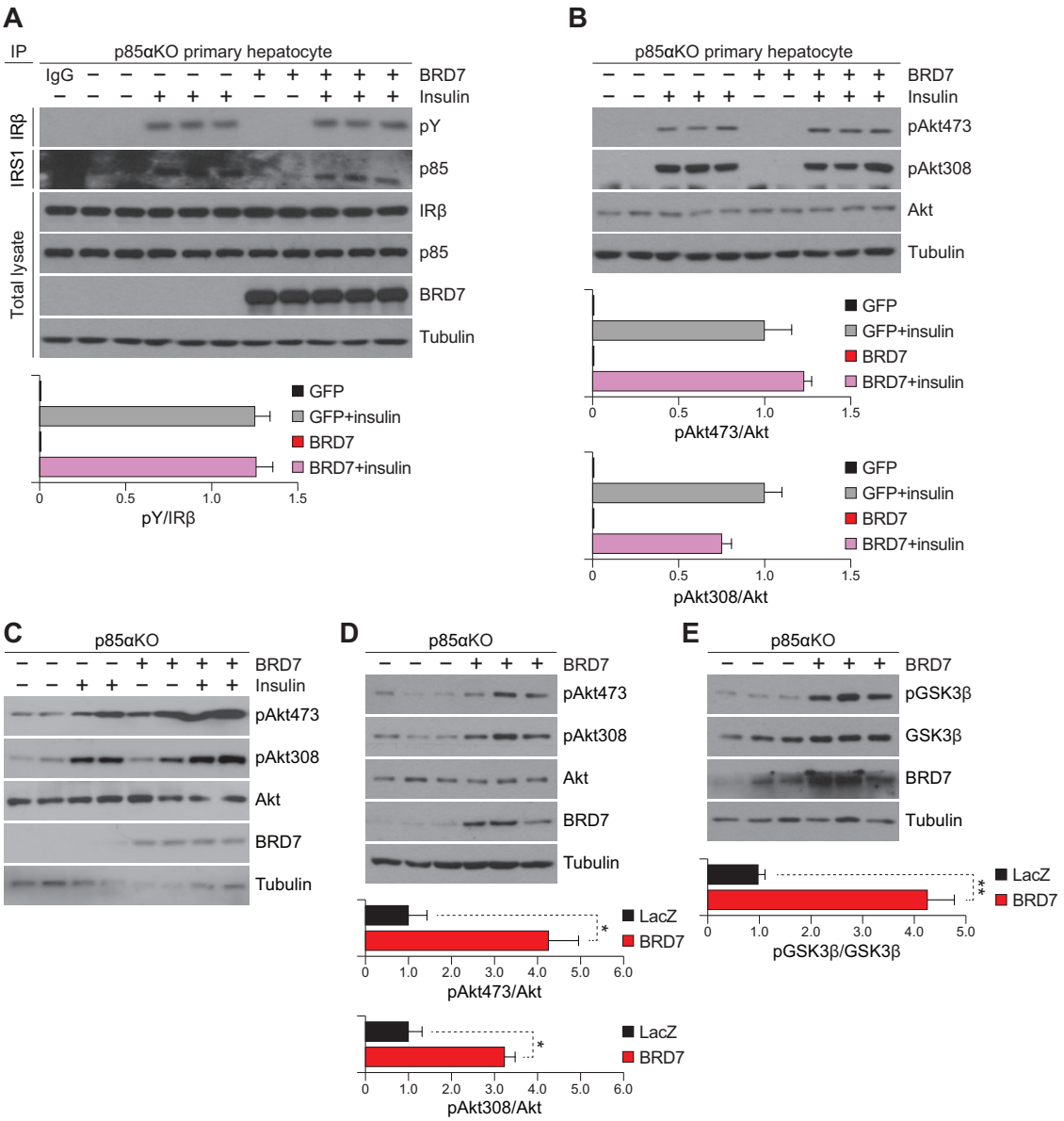

Figure 6 p85α is necessary for BRD7-mediated increase in Akt activation in response to insulin. Primary hepatocytes were isolated from p85αKO mice, infected with Ad-BRD7 or Ad-LacZ as a control, and stimulated with 100 nM insulin for 10 min. (**A**) Total cell lysates were IP with the indicated antibodies and immunoblotted with the indicated antibodies. (**B**) Western blotting was performed on total cell lysates with the indicated antibodies. (**C**–**E**) p85αKO mice were placed on HFD for 7–8 weeks starting at 4 weeks of age and injected with Ad-BRD7 or Ad-LacZ as a control through the tail vein at a dose of 1.0×10^8 pfu/g body weight. (**C**) On Day 8 postinjection, mice were fasted for 6 h and infused with insulin at a dose of 1.2 IU/kg body weight or saline as a control through the portal vein for 3 min. Western blotting was performed on total lysates from the liver with the indicated antibodies. (**D** and **E**) Phosphorylation levels of Akt and GSK3β in the liver on Day 9 postinjection after 6 h of fasting. For all graphs, Student's *t*-test was used to determine *P*-values. Error bars represent SEM. $*P < 0.05$. $**P < 0.01$.

(DMEM, Gibco, 11995065) with 10% fetal bovine serum (FBS, Gibco, 26140079), 10 U/ml penicillin, and 1 mg/ml streptomycin (Gibco, 15140122). The medium was changed to 1% FBS 16 h prior to experiments. Cells were maintained at 37°C in a humidified atmosphere with 5% CO_2.

Western blotting

Cells were lysed in RIPA buffer (25 mM Tris [pH 7.4], 10 mM NaF, 10 mM $Na_4P_2O_7$, 1 mM ethylenediaminetetraacetic acid (EDTA), 1 mM egtazic acid (EGTA), and 1% NP40) with phosphatase and protease inhibitor cocktail (Roche, 4906837001 and

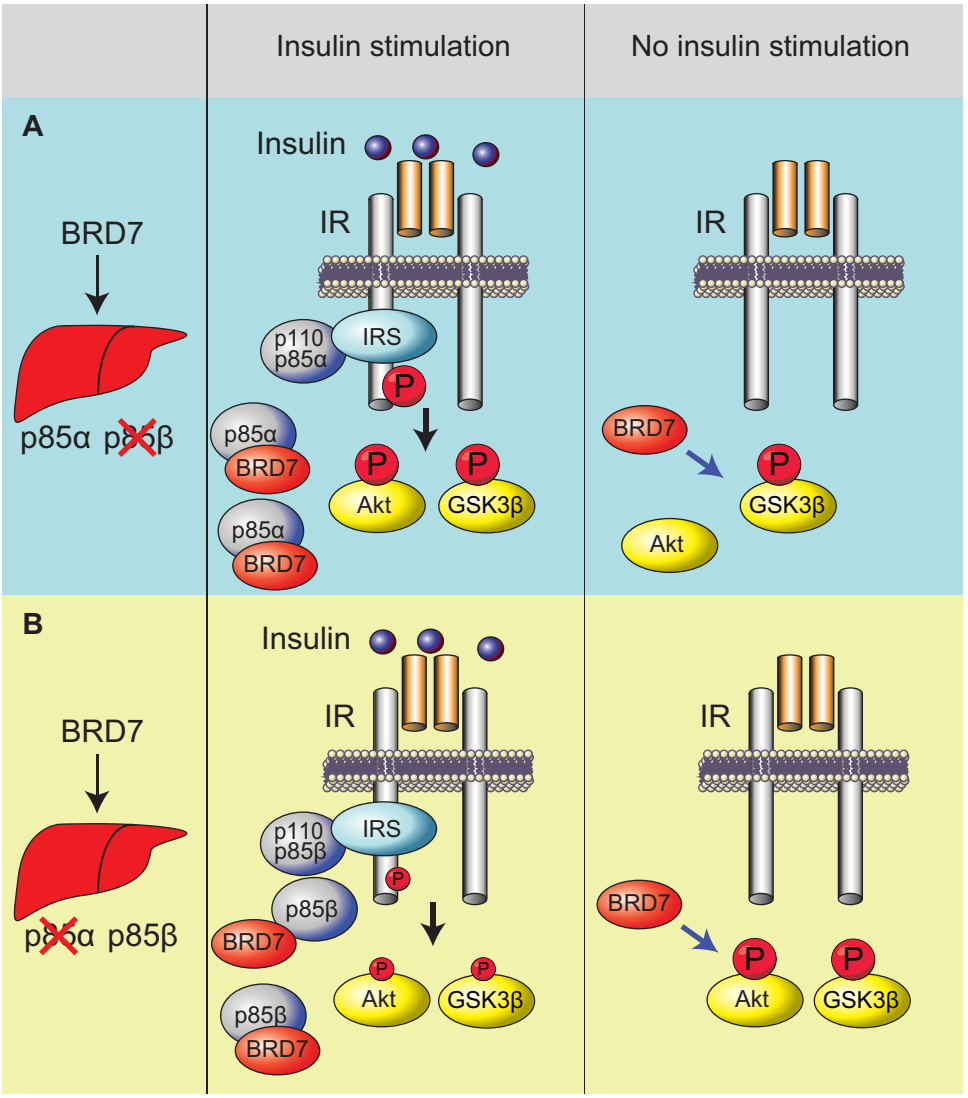

Figure 7 Schematic of the regulation of insulin signaling by BRD7 and p85. (**A**) In the presence of only p85α, BRD7 overexpression increases the sensitivity of the IR–IRS axis and insulin-induced phosphorylation of Akt. (**B**) In the presence of only p85β, BRD7 overexpression increases basal, but not insulin-induced, phosphorylation of Akt.

11836170001) for 10 min on ice. Total cell lysates were centrifuged at 16100× *g* for 5 min at 4°C. The supernatant was collected, and protein concentrations were measured using a Lowry assay kit (Bio-Rad, 5000112). Proteins were normalized and denatured in 1× Laemmli buffer (10% glycerol, 2% [*w*/*v*] sodium dodecyl sulfate (SDS), 50 mM Tris–HCl [pH 6.8], 4% β-mercaptoethanol, and 0.02% bromophenol blue), then boiled for 5 min at 100°C, and cooled to room temperature (RT). After resolving on an SDS–polyacrylamide gel electrophoresis (PAGE) gel, proteins were transferred onto a polyvinylidene fluoride membrane (Millipore Sigma, IVPH00010) and then incubated in Tris-buffered saline (TBS, pH 7.4) with 10% blocking reagent (Roche, 11921673001) for 1 h at RT. The membranes were then incubated with primary antibody in TBS-Tween 20 (TBS-T) with 5% blocking reagent overnight at 4°C. Membranes were then washed three times in TBS-T for 20 min per wash followed by incubation in secondary antibody in TBS-T with 5% blocking reagent for 1 h at RT. The membranes were washed three times for 20 min in TBS-T before visualization via chemiluminescence (Thermo Fisher, 34580) on autoradiography film (Hyblot, E3018). To obtain proteins from the liver, 5–20 mg of liver tissue was added to a round-bottom microcentrifuge tube containing a tungsten carbide bead (Qiagen, 69997) and 1 ml of ice-cold tissue lysis buffer (25 mM Tris–HCl [pH 7.4], 10 mM Na_3VO_4, 100 mM NaF, 50 mM $Na_4P_2O_4{\cdot}10H_2O$, 10 mM EGTA, 10 mM EDTA, and 1% NP40) with phosphatase and protease inhibitors. Tissue was homogenized by shaking for 2 min at 30 Hz in a tissue homogenizer (Qiagen, Tissue Lyser II). Samples were then incubated on a rotator for 1 h at 4°C followed by centrifugation at 16100× *g* for 1 h at 4°C. The lipid layer was carefully removed with a cotton swab and the supernatant was collected and processed as described above. For

western blotting results from *in vitro* experiments, each lane represents a plate of cells, performed as duplicates or triplicates. For *in vivo* experiments, each lane represents liver extracts of an individual mouse from the same cohort. Each experiment was repeated at least three times. Tubulin, Akt, GSK3β, pGSK3β (Ser9), pAkt (Thr308), pAkt (Ser473), phosphotyrosine, IRβ, p85, normal rabbit IgG, horseradish peroxidase (HRP)-linked goat anti-rabbit IgG, and HRP-linked horse anti-mouse IgG antibodies were obtained from Cell Signaling Technology. BRD7-specific antibody was custom produced by Covance Inc. Antibodies specific for IRS1 and IRS2 were generously provided by Dr Morris White.

Immunoprecipitation

To perform immunoprecipitation, protein lysates were incubated with antibodies on a rotator for 4 h at 4°C. Then, 30 µl of protein G Sepharose beads (GE Healthcare, 17061801) or 15–20 µl mixed protein A/G magnetic beads (MilliporeSigma, LSKMAGAG10) were added to lysates and rotated for additional 2 h at 4°C. Beads were washed three times with ice-cold lysis buffer, and pellets were collected by centrifuging at 2000× *g* for 2 min at 4°C for Sepharose beads or using magnets for magnetic beads. Next, 25–30 µl of 2× Laemmli buffer was added to the pellet and boiled for 5 min at 100°C. Samples were then resolved by SDS–PAGE and processed as described for western blotting.

RNA extraction and quantitative polymerase chain reaction (qPCR)

RNA was extracted from tissue samples using QIAzol lysis reagent according to the manufacturer's instruction (Qiagen, 79306). Extracted RNA was dissolved in nuclease-free water and cDNA was synthesized from 1 µg of RNA using a reverse transcription kit (Bio-Rad Laboratories, 1708890). The cDNA was diluted by 20 times in water, and qPCR was performed with SYBR Green (Applied Biosystems, A25778) using the QuantStudio 6 Flex Real-Time PCR system (Applied Biosystems) and the indicated primer sequences (Table 1).

Table 1 Primer sequences for qPCR.

Primer	Orientation	Sequences
18S	Forward	5′-AGTCCCTGCCCTTTGTACACA-3′
	Reverse	5′-CGATCCGAGGGCCTCACTA-3′
p85α	Forward	5′-GCGTCAGTGGACTTGGAGA-3′
	Reverse	5′-TGAAGCGTAAGCCAACACTG-3′
p85β	Forward	5′-CTCTCACACTGCGTTTCCTG-3′
	Reverse	5′-GAAGTCGGGTACAGGCTCAC-3′
BRD7	Forward	5′-GAGGCTGAGGTGTTCCAGAG-3′
	Reverse	5′-TCACCTGGAGTCACTTGCTG-3′
G6P	Forward	5′-CCGGTGTTTGAACGTCATCT-3′
	Reverse	5′-CAATGCCTGACAAGACTCCA-3′
F6P	Forward	5′-CTTTTTATACCCCGCCAACA-3′
	Reverse	5′-TCTTCAGAGGACCCCATGAC-3′
PEPCK	Forward	5′-TGACATTGCCTGGATGAAGT-3′
	Reverse	5′-GTCTTAATGGCGTTCGGATT-3′

Adenovirus production

Mouse BRD7 cDNA (NCBI Reference Sequence NM_012047.2) was cloned into pENTR3C (Invitrogen, A10464) and then recombined into pAD-CMV-DEST (Invitrogen, V49320) using the Gateway cloning system (Invitrogen, 11791020). The recombined pAd-BRD7 was used to produce the first generation of adenovirus (Ad-BRD7) as described previously (Golick et al., 2018). To produce Ad-p85α-HA, Ad-p85β-HA, pENTR3C-p85α, and pENTR3C-p85β (Park et al., 2014), plasmids were amplified by PCR using the following HA-tagged primers: p85α-HA forward 5′-TACCCATACGATGTTCCAGATTACGCTAGTGCAGAGGGCTAC-3′; p85α-HA reverse 5′-TCATCGCCTCTGTTGTGCATATA-3′; p85β-HA forward 5′-TACCCATACGATGTTCCAGATTACGCTGCAGGAGCCGAGGGCTTC-3′; p85β-HA reverse 5′-TCAGCGTGCTGCAGACGGTGGGCC-3′. The resulting pENTR3C-p85α-HA and pENTR3C-p85β-HA plasmids were recombined into pAD-CMV-DEST using the Gateway cloning system to produce the first generation of adenovirus (Golick et al., 2018). To produce subsequent generations of adenovirus, 293A cells were infected with adenovirus in DMEM with 5% FBS, 10 U/ml penicillin, and 1 mg/ml streptomycin and incubated until the cytopathic effect was observed in 80% of cells. Cells were collected and centrifuged at 225× *g* for 3 min. The pellet was resuspended in DMEM with 1% FBS, 10 U/ml penicillin, and 1 mg/ml streptomycin. The resuspension volume was calculated as 5.7 µl/cm^2 of infected cells. Cells were lysed by three cycles of freezing in liquid nitrogen and thawing at 37°C. The lysate was centrifuged at 3000× *g* for 20 min, and the supernatant containing viral particles was collected and stored at −80°C. Absorbance at 260 nm was measured using a fluorescence spectrophotometer (Thermo Scientific, ND-3300) to determine infection dosage for *in vitro* experiments.

Mouse lines and husbandry

C57BL/6J mice were purchased from The Jackson Laboratory. Liver-specific p85αKO (L-p85α$^{F/F}$Cre$^{+/-}$) mice were generated by first crossing p85α$^{F/F}$p85β$^{-/-}$ mice obtained from Dr Lewis Cantley with wild-type mice to create p85α$^{F/F}$p85β$^{+/+}$ mice, and then breeding p85α$^{F/F}$p85β$^{+/+}$ mice with a mouse line that expresses Cre recombinase under a modified human albumin promoter obtained from The Jackson Laboratory. Genotypes were determined by standard PCR procedures using DNA extracted from tail biopsies. Mice were grouped at the time of weaning only according to their genotypes. Mice were fed on either an NCD (LabDiet 5P76) or irradiated HFD (Research Diets Inc. D12451i) and housed in a temperature- and humidity-controlled environment under a 12-h light (7 am–7 pm) and dark (7 pm–7 am) cycle. All experimental animal procedures were performed identically regardless of animal genotypes or diet. All experiments were performed during the light cycle. All

experiments were approved by Institutional Animal Care and Use Committee (IACUC) at Boston Children's Hospital.

Adenovirus injection

Ad-LacZ (Vector Biolabs, 1080-HT) or Ad-BRD7 for *in vivo* use was purified by Vector Biolabs using cesium chloride density gradient. The plaque-forming unit (pfu) of viruses and viral particle number were provided by Vector Biolabs. The purified virus was diluted in saline to a volume of 100 μl per mouse before injection. Mice were placed in a restrainer and injected with the adenovirus solution through the tail vein or retro-orbitally after isoflurane anesthesia (Patterson Veterinary, 14043-704-05). Mild pressure was applied to the injection site following injection to prevent the backflow of virus.

GTT and ITT

To perform a GTT, mice were fasted during the dark cycle for 14 h (7 pm–9 am). Prior to administration of glucose, fasting blood glucose levels were measured from the tail using a commercial blood glucose meter (Bayer, 9545C). For each mouse, 1.5 g of glucose (Hospira, 0409-6648-02) per kg body weight, diluted in saline (Hospira, 0409-4888-03) to a volume of 100–150 μl, was administered via intraperitoneal injection. Blood glucose levels were measured at 15-, 30-, 60-, 90-, and 120-min postinjection. ITTs were performed similarly, except that mice were fasted during the light cycle for 6 h (8 am–2 pm) and injected with 1.0–1.5 IU of recombinant human insulin (Eli Lilly) that was diluted in saline to a volume of 100 μl.

Primary hepatocyte isolation

To prepare collagen-coated plates, 4 ml of a solution consisting of 20 mM acetic acid and 20 μg/ml collagen type I (Corning, 354236) was added to 6-cm tissue-culture treated plates and incubated overnight in a fume hood. Plates were washed twice with 1× PBS (Gibco, 10010023). After anesthetizing mice with 120 mg ketamine (Vedco, 50989-161-06) and 10 mg xylazine (Akorn, 59399-110-20) per kg body weight, 50 ml of prewarmed perfusion solution (1× Hank's buffered salt solution [HBSS, Gibco, 14185052], 0.5 mM EGTA, 5.5 mM glucose, 10 U/ml penicillin, and 1 mg/ml streptomycin) was infused into the liver through the portal vein at a rate of 5.5 ml/min using a perfusion pump. The inferior vena cava was immediately cut to release pressure at the start of perfusion. Consequently, 40 ml of prewarmed digest solution (375 μg/ml collagenase, 1× HBSS, 1.5 mM $CaCl_2$, 5.5 mM glucose, 10 U/ml penicillin, and 1 mg/ml streptomycin) was perfused at the same rate. Following perfusion, the liver was placed into a petri dish containing prewarmed digest solution and mechanically dissociated using tweezers. Cells were filtered through a 70-μm filter and centrifuged at 400× *g* for 4 min at 4°C. The pellet was resuspended in 4°C solution consisting of 1 ml of 10× HBSS, 9 ml of Percoll (GE Healthcare, 17089102), and 8 ml of DMEM with 10 U/ml penicillin and 1 mg/ml streptomycin, followed by centrifugation at 400× *g* for 8 min at 4°C. The pellet was washed twice with ice-cold DMEM, resuspended in 5–10 ml of prewarmed DMEM with 10% FBS, 10 U/ml penicillin, and 1 mg/ml streptomycin, and then plated onto collagen-coated plates.

Quantification and statistical analysis

Western blotting quantifications represent average band intensity, which was determined using ImageJ. Statistical analysis was performed only for blots with a sample number of 3 or greater. For blots with a sample number of 2, individual band intensities were dot plotted on quantifications. Western blotting quantification, blood glucose, and AUC data were analyzed by Student's *t*-test. Group differences in GTT and ITT were analyzed by two-way repeated measure analysis of variance (ANOVA). Error bars represent SEM. Significance was presented at $*P < 0.05$, $**P < 0.01$, $***P < 0.001$.

Supplementary material

Supplementary material is available at *Journal of Molecular Cell Biology* online.

Acknowledgements

We thank Dr L.C. Cantley (Weill Cornell Medicine) for initially providing us with the $p85\alpha^{F/F}p85\beta^{-/-}$ mice and for his useful discussion, Dr M. White (Boston Children's Hospital and Harvard Medical School) for providing IRS1 and IRS2 antibodies, Dr R.C. Kahn's group (Joslin Diabetes Center, Harvard Medical School) for kindly providing the p85 double knockout cell line, and Dr T. Kim (Boston Children's Hospital, Harvard Medical School) for his contribution in isolating primary hepatocytes and performing western blotting.

Funding

This work was supported by the National Institutes of Health (R01DK118244), the American Heart Association (18IPA34140057), the American Diabetes Association (1-17-IBS-104), and the faculty start up fund provided to S.W.P. from Boston Children's Hospital.

Conflict of interest: none declared.

Author contributions: J.M.L. performed the experiments, analyzed and interpreted the data, and wrote the manuscript. R.L. performed the experiments. S.W.P. interpreted the data and wrote the manuscript. The data and material that support the finding of this study are available from the corresponding author, S.W.P., upon reasonable request.

References

Bandyopadhyay, G.K., Yu, J.G., Ofrecio, J., et al. (2005). Increased p85/55/50 expression and decreased phosphotidylinositol 3-kinase activity in insulin-resistant human skeletal muscle. Diabetes *54*, 2351–2359.

Burrows, A.E., Smogorzewska, A., and Elledge, S.J. (2010). Polybromo-associated BRG1-associated factor components BRD7 and BAF180 are critical regulators of p53 required for induction of replicative senescence. Proc. Natl Acad. Sci. USA *107*, 14280–14285.

Cheung, L.W., Walkiewicz, K.W., Besong, T.M., et al. (2015). Regulation of the PI3K pathway through a p85α monomer–homodimer equilibrium. eLife *4*, e06866.

Chiu, Y.-H., Lee, J.Y., and Cantley, L.C. (2014). BRD7, a tumor suppressor, interacts with p85α and regulates PI3K activity. Mol. Cell *54*, 193–202.

DeFronzo, R.A., Ferrannini, E., Groop, L., et al. (2015). Type 2 diabetes mellitus. Nat. Rev. Dis. Primers *1*, 15019.

Drost, J., Mantovani, F., Tocco, F., et al. (2010). BRD7 is a candidate tumour suppressor gene required for p53 function. Nat. Cell Biol. *12*, 380–389.

Forbes, J.M., and Cooper, M.E. (2013). Mechanisms of diabetic complications. Physiol. Rev. *93*, 137–188.

Golick, L., Han, Y., Kim, Y., et al. (2018). BRD7 regulates the insulin-signaling pathway by increasing phosphorylation of GSK3β. Cell. Mol. Life Sci. *75*, 1857–1869.

Gomez-Hernandez, A., Lopez-Pastor, A.R., Rubio-Longas, C., et al. (2020). Specific knockout of p85α in brown adipose tissue induces resistance to high-fat diet-induced obesity and its metabolic complications in male mice. Mol. Metab. *31*, 1–13.

Harte, M.T., Brien, G.J., Ryan, N.M., et al. (2010). BRD7, a subunit of SWI/SNF complexes, binds directly to BRCA1 and regulates BRCA1-dependent transcription. Cancer Res. *70*, 2538–2547.

Lee, J.M., Kim, Y., Salazar Hernández, M.A., et al. (2019). BRD7 deficiency leads to the development of obesity and hyperglycemia. Sci. Rep. *9*, 5327.

Luo, J., Field, S.J., Lee, J.Y., et al. (2005). The p85 regulatory subunit of phosphoinositide 3-kinase down-regulates IRS-1 signaling via the formation of a sequestration complex. J. Cell Biol. *170*, 455–464.

Mantovani, F., Drost, J., Voorhoeve, P.M., et al. (2010). Gene regulation and tumor suppression by the bromodomain-containing protein BRD7. Cell Cycle *9*, 2777–2781.

Mauvais-Jarvis, F., Ueki, K., Fruman, D.A., et al. (2002). Reduced expression of the murine p85α subunit of phosphoinositide 3-kinase improves insulin signaling and ameliorates diabetes. J. Clin. Invest. *109*, 141–149.

Oak, J.S., Chen, J., Peralta, R.Q., et al. (2009). The p85β regulatory subunit of phosphoinositide 3-kinase has unique and redundant functions in B cells. Autoimmunity *42*, 447–458.

Park, S.W., Herrema, H., Salazar, M., et al. (2014). BRD7 regulates XBP1s' activity and glucose homeostasis through its interaction with the regulatory subunits of PI3K. Cell Metab. *20*, 73–84.

Park, S.W., and Lee, J.M. (2020). Emerging roles of BRD7 in pathophysiology. Int. J. Mol. Sci. *21*, 7127.

Park, S.W., and Ozcan, U. (2013). Potential for therapeutic manipulation of the UPR in disease. Semin. Immunopathol. *35*, 351–373.

Park, S.W., Zhou, Y., Lee, J., et al. (2010). The regulatory subunits of PI3K, p85α and p85β, interact with XBP-1 and increase its nuclear translocation. Nat. Med. *16*, 429–437.

Taniguchi, C.M., Tran, T.T., Kondo, T., et al. (2006). Phosphoinositide 3-kinase regulatory subunit p85α suppresses insulin action via positive regulation of PTEN. Proc. Natl Acad. Sci. USA *103*, 12093–12097.

Ueki, K., Fruman, D.A., Brachmann, S.M., et al. (2002). Molecular balance between the regulatory and catalytic subunits of phosphoinositide 3-kinase regulates cell signaling and survival. Mol. Cell. Biol. *22*, 965–977.

Vallejo-Diaz, J., Chagoyen, M., Olazabal-Moran, M., et al. (2019). The opposing roles of PIK3R1/p85α and PIK3R2/p85β in cancer. Trends Cancer *5*, 233–244.

Wei, Z., Yoshihara, E., He, N., et al. (2018). Vitamin D switches BAF complexes to protect β cells. Cell *173*, 1135–1149.e15.

Winnay, J.N., Dirice, E., Liew, C.W., et al. (2014). p85α deficiency protects β-cells from endoplasmic reticulum stress-induced apoptosis. Proc. Natl Acad. Sci. USA *111*, 1192–1197.

Zhou, J., Ma, J., Zhang, B.-C., et al. (2004). BRD7, a novel bromodomain gene, inhibits G1–S progression by transcriptionally regulating some important molecules involved in ras/MEK/ERK and Rb/E2F pathways. J. Cell. Physiol. *200*, 89–98.